Zagazig University Medical Journal
www.zumj.journals.ekb.eg
https://doi.org/10.21608/zumj.2024.318727.3566 Volume 31, Issue 1, January. 2025
Manscript ID: ZUMJ-2409-3566
DOI: 10.21608/ZUMJ.2024.318727.3566

ORIGINAL ARTICLE

Modulatory effects of pycnogenol and L-arginine administrations on the uterine and ovarian histological alterations provoked by Thiamethoxam in Adult rat models

Samar Fawzy Gad, Marim Fayz Abdo
Lecturer of Anatomy and Embryology, Faculty of Medicine, Benha University, Egypt

Corresponding author:
Samar Fawzy Gad

E-mail:
samar.gad@fmed.bu.edu.eg

Submit date: 10-09-2024
Revise date: 24-10-2024
Accept date: 27-10-2024

ABSTRACT

Background: Thiamethoxam (TMX) is a widespread neonicotinoid insecticide; it thought to have a toxic effect on uterine and ovarian tissue. This experiment aimed to evaluate the possible antioxidant protective role of both the pycnogenol and L-arginine against this damage using histological, immunohistochemical, and morphometric analysis.

Methods: Forty eight female albino rats were randomly divided into 4 groups; twelve rats per group as follows: 312 mg/kg thiomethoxame group (Tx group), 40 mg/kg pycnogenol + 312 mg/kg thiomethoxame group (Tx /Pg group), 1.3 g/kg L-arginine +312 mg/kg thiomethoxame group ((Tx /La group), and a healthy control group. The rats were supplied with L-arginine, Pycnogenol, TMX, and distilled water once a day for 30 days then sacrificed. Ovarian and uterine tissues were removed for biochemical and histological analysis.

Result: A decrease in the activities of glutathione (GSH), catalase (CAT), and superoxide dismutase (SOD) and increasing malondialdehyde (MDA) levels in Tx group, TMX caused a marked oxidative stress. Also, tissue damage in the same group appeared in the form of atretic and vacuolated ovarian follicles with degenerated uterine gland. Immunohistochemistry data, showed elevated level of cytoplasmic reactivity to caspase3 with decrease reaction to Nfr2 in Tx group as compared to other groups. Pycnogenol and L-arginine administration revealed significant restoration of normal histological and immunohistochemical tissue form**.**

Conclusion: The present findings suggest that Pycnogenol and L-arginine could improve the ovarian and uterine damage resulting from administration of thiomethoxame.

Keywords: Thiamethoxam, Pycnogenol, L-arginine, ovary, uterus, oxidative stress.

INTRODUCTION

Neonicotinoids are organic pesticides that are extremely soluble in water and are used in more than 120 countries [1].Neonicotinoids were formerly thought to have a brief biological half-life; but they are frequently discovered in the soil of lands that have been treated to grow a range of crops. Their concentrations in the soil rise following repeated application, and they can be found in the environment for up to 18 years [2]. Specifically, neonicotinoids operate as strong agonists of nicotinic acetylcholine receptors in target insects, which cause neurotoxicity in the insects. Mammals and aquatic species are at non-selective risk Thiamethoxam (TMX) is a systemic insecticide of the neonicotinoid class [3].

In vitro, TMX might be detrimental to the reproductive health of mammals as it damages DNA, modifies the activity of antioxidant enzymes, and initiates lipid peroxidation (LPO) malondialdehyde (MDA) [4].Due to its extensive usage today, it also has detrimental effects on cardiac, hepatic, renal, and testicular functioning [5]. Loser et al [6]stated that, mammals exposed to TMX, their brain tissues contain the metabolites around 50% of the parent chemical. These metabolites have a cationic nature and are hence selective for the mammalian nAChRs, making the possible consequences on mammals quite intriguing. Also, free radicals produced by TMX and its metabolites weaken antioxidant

capacity to shield the body from these toxins and cause oxidative stress [7].

Naturally occurring flavonoids exhibit the capacity to regulate intracellular signals, hence providing neuroprotection against oxidative injury and free radical scavenging activities [9].These flavonoids can be found in fruits, vegetables, and drinks made from plants. They may play significant roles in diets by acting as cytoprotectors in a variety of organs [9].Pycnogenol (PYC) is a patented blend of bioflavonoids made from the bark of the French coastal pine Pinus maritima. It is produced using a standardized procedure [10].Using ethanol and water, fresh pine bark is extracted in this process [11]. The bulk of this combination is composed of procyanidins, flavonoids, phenolic compounds, phenolic or cinnamic acids and their glycosides, and procyanidins [12].

Additionally, PYC has been demonstrated to have positive benefits on menstrual, cardiovascular, skin, and cognitive disorders. It has also been demonstrated to have positive effects when combined with other illnesses and disease processes like diabetes, asthma, and inflammation [14]. Numerous in vitro and cell culture investigations have clarified the processes behind these effects of PYC extract [10]. Apart from its ability to scavenge free radicals, the pycnogenol extract was found to suppress gene expression that is dependent on NF-κB and to lower the activity of several pro-inflammatory mediators and adhesion molecules in cells that were incubated with it [9].

The female reproductive system may be severely disrupted by TMX treatment, resulting in changes to granulosa cell-mediated hormone synthesis in the ovarian follicles, oogenesis, ovulation, and the shape and function of accessory reproductive structures (the oviduct, uterus, and vagina) [14].

METHODS

Chemicals

Thiamethoxam (TMX): having the chemical name 3-(2-chloro-thiazol-5-ylmethyl)-5-methyl-[1, 3, 5] oxadiazinan-4-ylidene-N-nitroamine, ACTARA® 25WG (Syngenta Canada Inc.) was commercially available from the local pesticide market. Distal water was used as solvent.

Pycnogenol (Nature Way Company, the United States): containing 30 Vegan Tablets. Each tablet has fifty milligrams of pure pycnogenol powder. Pycnogenol extract, was dissolved in distal water.

L-arginine tablets (NOW Foods Company, Bloomingdale, IL, USA): containing 120 tablets, each tablet has 1000 mg. It was prepared by dissolving it in distilled water.

Animals

The animal house at Cairo University, Faculty of Veterinary Medicine, Egypt, provided forty eight female Albino rats about 240 gram weight. The rats were housed for a week to allow them to acclimate at the Anatomy Department of Benha Faculty of Medicine, with laboratory conditions set at 20 to 25 °C and a 12-hour light/dark cycle (Ethical approval No. RC 12-1-2024)

EXPERIMENTAL DESIGN

The rats were divided as follows:

Group I (Control group): twelve rats were divided into three subgroups:

Subgroup a: included four adult female albino rats received distal water.

Subgroup b: included four adult female albino rats, administered 40 mg/kg Pycnogenol by oral gavage daily [12].

Subgroup c: included four adult female albino rats received L-arginine at a dose 1.3 g/kg injection intraperitoneally daily [15].

Group II (Tx group): twelve adult female albino rats received 312 mg/kg TMX, by oral gavage daily [1].

Group III (Tx /Pg group): twelve adult female albino rats received TMX (312 mg/kg by oral gavage) one hour after administration of the pycnogenol (as mentioned in subgroup Ib).

Tx /La group (Tx /La group): twelve adult female albino rats received TMX (312 mg/kg by oral gavage) one hour after administration of L-arginine (as mentioned in subgroup Ic).

For thirty days, the prescribed doses of L-arginine, Pycnogenol, TMX, and distilled water will be administered once daily. All rats were sacrificed by intraperitoneal injection of 50 mg/kg thiopental sodium. Their ovarian and uterine tissues were extracted.

Biochemical analysis of uterine and ovarian tissues

Using Tris-HCl (5 mmol/l containing 2 mmol/l EDTA, pH 7.4), the ovary and uterus were homogenized. The homogenate was then centrifuged at 1,000 ×g for 10 minutes at 40°C. Using Bradford's (1976) [16] technique, supernatants were utilized to measure antioxidant biomarkers and oxidative stress marker. Lipid peroxidation (MDA; ab118970, Abcam) is a colorimetric/fluorometric measurement that is based on the amount of malondialdehyde generated during the breakdown of polyunsaturated fatty acids. Furthermore, the amount of superoxide dismutase activity (SOD antioxidant enzyme) (Colorimetric; ab65354, Abcam) was determined. The amount of antioxidant enzyme known as CAT (catalase activity) (Colorimetric/Fluorometric; ab83464;

Abcam) was ascertained by monitoring the breakdown of the hydrogen peroxide enzyme catalyzed by potassium permanganate. GSH activity was measured colorimetrically using kits for the GSH test (Colorimetric; ab283966, Abcam).

HISTOPATHOLOGICAL STUDIES

After preservation of ovarian and uterine tissues for 48 hours in a 10% formalin solution. After being run through a succession of alcohol, the tissues were embedded in paraffin blocks. From each block, 5 µm thick sections were cut and subjected to Hematoxylin and eosin (H&E) staining. [17].

Immunohistochemical examination

On positively charged slides, 5 µm thick sections were immunostained with an avidin-biotin method. The sections were deparaffinized, rehydrated, and exposed to 0.01 percent hydrogen peroxide (H2O2) to suppress endogenous peroxidase activity. Also, the sections were subjected to antigen retrieval and blocking the non-specific binding sites. The sections were then incubated with primary antibodies with appropriate dilutions [18].

Caspase-3 (CAT-No: 43-7800; ThermoFisher) and Nrf2 (CAT-No: PA5-27882; ThermoFisher) primary antibodies were utilized (Nrf2 antimouse monoclonal antibody, 1:100 dilution; caspase 3 anti-mouse polyclonal, 1:10 dilution). After that, the sections were incubated with biotinylated secondary antibody and streptavidin peroxidase complex with application of chromogen diaminobenzidine solution.

Finally, a counter stain of Mayer's hematoxylin was utilized. For both antigens, immunoreactivity was seen in the nucleus. The particular 1ry antibody was substituted with phosphate buffer saline for the negative control slide. Positive cells for caspase-3 and Nrf2 appear with brown cytoplasmic staining and may also show nuclear staining.

H & E and Immunohistochemical sections were examined and photographed using light microscope (Olympus CX 41, Japan) with an attached camera (Olympus E 330, Japan) at Anatomy and Embryology Department, Faculty of Medicine, Benha University.

Morphometric analysis

For morphometric analysis, ten non-overlapping fields in three non-serial Immunohistochemical-stained ovarian and uterine sections from each group were examined. The area percentage of Caspase 3 and Nrf2 positive expression in the Immunohistochemical-stained sections at 200 × magnifications was determined using the Image J software analyzer computer.

Statistical analysis:

The mean and standard deviation were used to summarize the data for MDA, GSH, SOD, and CAT levels, as well as the area percentage of Caspase 3 and Nrf2 positive expression. The study employed analysis of variance (ANOVA) to investigate potential discrepancies in mean values among the experimental groups. A post hoc Tukey's test is used to compare the difference between each pair of means. The 5% level (P value) is the set threshold of significance. A value of $p < 0.05$ was deemed statistically significant, whereas a value of $p > 0.05$ was deemed non-statistically significant.

RESULT

Biochemical analysis of ovarian tissue

MDA, GSH, SOD, and CAT levels were measured to assess the oxidative state of ovarian tissue in both treated and control rats (table 1). It was shown a significant increase in MDA level of Tx group and Tx /La group compared to control group, while MDA level showed significant decrease in Tx /Pg group and Tx /La group compared to Tx group.

Compared to control group, GSH, SOD and CAT levels were significantly decreased in Tx group, Tx /Pg group and Tx /La group. However, GSH, SOD and CAT levels had significant increase in Tx /Pg group and Tx /La group compared to Tx group.

Biochemical analysis of uterine tissue

MDA, GSH, SOD, and CAT levels (table 1) were measured to assess the uterine tissue oxidative state in both treated and control rats. MDA levels have shown significant increase in Tx group and Tx /La group comparing to control group. While MDA levels were significantly decreased in Tx /Pg group and Tx /La group compared to Tx group.

In comparison to the control group, the Tx group, Tx /Pg group, and Tx /La group all showed significant decrease levels of GSH, SOD, and CAT. While these parameters had significant increase in Tx /Pg group and Tx /La group compared to Tx group. There was a significant decrease in GSH and SOD levels in Tx /La group compared to Tx /Pg group.

Ovarian Histological Examination

Under a light microscope, H&E-stained ovarian sections in the control group showed that, thick capsule of connective tissue called the tunica albuginea encircles the ovary. A single layer of cuboidal, germinal epithelium covers the surface of the tunica albuginea. At varying stages of maturation, typical ovarian follicles were seen in the cortical stroma. An oocyte encircled by

follicular cells formed each follicle. The medulla showed signs of normalcy, with fibroblast and interstitial cells dividing its regular vascularity (Fig. 1a). The oocyte encircled by granulosa cells, theca externa and interna, and antral space was seen in the Graffian follicle (Fig.1b)

The ovarian sections of Tx group showed atrophic and degenerative ovarian changes. Many atretic primordial, secondary, and graffian follicles were seen together with dilated, congested blood vessels. There were loose granulosa cells with apoptotic nuclei and degenerated oocytes in the atretic follicles. There were vacuolated granulosa cells with pyknotic nuclei and a seemingly degenerated corpus luteum (Fig. 2a, b).

The histological structure of the ovary improved in all specimens as a result of the pycnogenol treatments. In the ovarian sections of Tx /Pg group, During various phases of development, intact follicles were seen. The secondary follicle had normal granulosa cells surrounded apparently normal oocyte. There were interstitial vacuolar changes and marked congested blood vessels with highly cellular infiltration (Fig. 3a, b).

The ovarian structure in the Tx/La group was closely resembled that of the control group. Ovarian follicles at various stages were observed and had a consistent structure. There were no atretic follicles and little vacuolar alterations in the interstitial cells (Fig. 4a, b).

Uterine histopathological Examination

Upon examining H&E-stained sections of the control group, it was seen that columnar epithelial cells lining the uterine cavity comprised the endometrium in all subgroups of control rats. The surface epithelial cells were composed of ciliated and secretory simple columnar cells with an extended pale spherical nucleus. Long, tubular uterine glands lined by simple columnar epithelial cells with ciliated cells. It proceeds downward into the lamina propria connective tissue (stroma). A dense, well-organized population of stromal cells was present in the endometrial stroma as leukocytes with segmented nuclei and deep acidophilic cytoplasm, large cells with round nuclei, and spindle-shaped cells with dark stained nuclei (fibroblast-like cells) (Fig.5a, b).

Sections of the Tx group showed that the endometrial structure was affected. The cubical cells with dark stained nuclei were predominant in the surface epithelium. There were cytoplasmic vacuolations. The stroma seemed thick, and the endometrial glands were few, tiny, round, and ill-defined. The nuclei of the glandular epithelium were strongly pigmented, spherical, and vacuolated. Also, vacuolated cytoplasm and darkly pigmented nuclei were seen in some stromal cells. There were dilated congested blood vessels and spaces in stroma can be observed (Fig. 6a, b).

The majority of the surface epithelium in the Tx/Pg group H&E-stained sections had tall, columnar ciliated cells with round, vesicular nuclei. The endometrial stroma became dense. The glands were encircled by spindle-shaped cells and many rounded cells. The size and form of the endometrial glands returned to normal. They were round, and numerous. Large, spherical vesicular nuclei were seen in the glandular epithelial cells. Certain cells underwent apoptotic alterations, and chromatin-marginalized nuclei were also seen (Fig. 7a, b).

Sections of the endometrium taken from animals in the Tx/La group showed cubical cells with rounded nuclei. The thick stroma was mostly made up of spindle-shaped cells. In addition, a large number of cells with round nuclei were seen. The majority of the glands seemed to be round and little. The glandular epithelium had vesicular round nuclei. Atrophied glands often took the form of solid cell cords. Some of the glandular epithelium had vacuolated cytoplasm and deep stained nuclei (Fig. 8a, b).

Immunohistochemical observations of the ovary

Caspase-3 immunohistopathological analysis of ovarian tissue from the control group revealed minimal cytoplasmic positivity. Sections from TX group showed obvious cytoplasmic reaction which were significantly improved in Tx /Pg group and Tx /La group. Tx group, Tx /Pg group and Tx /La group had significantly higher Caspase-3 staining compared to control group. However, it showed significant decrease of Caspase-3 positive expression in Tx /Pg and Tx /La group when compared with Tx groups (table 2, Fig. 9).

Nrf2 immunohistopathological study of control group localized to cytoplasm of luteal cells and granulosa cells was observed. Ovaries in Tx group showed significantly decrease in positive area of Nrf2 compared with control group, Tx /Pg group and Tx /La group. Nrf2 staining was significantly increased in Tx /Pg group and Tx /La group when compared to control group (table 2, Fig. 10).

Immunohistochemical observations of the uterine tissue

In uterine tissue,Caspase-3 immune histopathological analysis of the control group revealed minimal cytoplasmic positivity. The TX group exhibits an extensive cytoplasmic response in endometrial, glandular epithelium, and stroma cells, which were ameliorated in the Tx/Pg and Tx/La groups (Fig.11). Tx group, Tx /Pg group and Tx /La group had significantly higher

Caspase-3 staining compared to control group while it showed significant decrease in Caspase-3 expression of Tx /Pg group and Tx /La group comparing with Tx group (table 2).

Nrf2 immunohistopathological study of control group localized to cytoplasm of surface epithelium, glandular epithelium and stroma cells was observed. Sections in Tx group showed decrease in positive area of Nrf2 while it was more obvious in uterine sections of Tx /Pg group and Tx /La group (Fig.12). In Tx group, it showed significantly decrease in positive area of Nrf2 compared with control group. However, it showed significant increase of Nrf2 positive expression in Tx /Pg and Tx /La group when compared with Tx groups. Also, it showed significant increase of Nrf2 positive expression in Tx /Pg comparing with control group and Tx /La group (table 2).

TABLE 1:ANOVA is used to examine the data, which are shown as Mean values ± SD of the levels of MDA, GSH, SOD, and CAT in the ovarian tissue and the uterine tissue of control and experimental groups

		Control group	Tx group	Tx /Pg group	Tx /La group	P value
MDA (micromol/g of protein)	Mean ± SD	5.9±1.02	23.5±2.13	7.8±1.46	9.4±0.66	<0.001*
	Range	4.6 – 7	20.8 - 25.9	6.5 - 9.3	8.5 - 10.1	
Post hoc		P1	<0.001*	0.081	0.001*	
		P2		<0.001*	<0.001*	
		P3			0.093	
GSH (nanomol/g of protein)	Mean ± SD	7.2±0.52	2.6±0.67	5.3±1.22	5±0.58	<0.001*
	Range	6.8 - 7.9	1.8 - 3.4	3.9 - 6.6	4.4 - 5.5	
Post hoc		P1	<0.001*	0.03*	0.001*	
		P2		0.009*	0.002*	
		P3			0.673	
SOD (U/g of protein)	Mean ± SD	14±1.21	3.9±0.46	10.8±0.83	10.7±0.47	<0.001*
	Range	12.3 - 15.1	3.4 - 4.5	9.6 - 11.6	10.4 - 11.4	
Post hoc		P1	<0.001*	0.004*	0.001*	
		P2		<0.001*	<0.001*	
		P3			0.92	
CAT (U/mg of protein)	Mean ± SD	18±0.51	9.6±0.84	16.3±0.75	16.2±0.54	<0.001*
	Range	17.3 - 18.5	8.8 - 10.8	15.6 - 16.9	15.4 - 16.5	
Post hoc		P1	<0.001*	0.008*	0.001*	
		P2		<0.001*	<0.001*	
		P3			0.917	
Uterine tissue						
MDA (micromol/g of protein)	Mean ± SD	5.1±1.43	20±2.6	5.8±2.34	10.1±1.67	<0.001*
	Range	3.6 - 7	17.2 - 23.2	3.5 - 8.7	8.5 - 12.4	
Post hoc		P1	<0.001*	0.665	0.001*	
		P2		<0.001*	<0.001*	
		P3			0.023*	
GSH (nanomol/g of protein)	Mean ± SD	52.6±1.41	25.6±2.16	44.8±2.94	34.8±1.26	<0.001*
	Range	50.7 - 54	22.7 - 27.8	40.9 - 47.8	33.5 - 36	
Post hoc		P1	<0.001*	0.003*	0.001*	
		P2		<0.001*	<0.001*	
		P3			<0.001*	
SOD (U/g of protein)	Mean ± SD	29.4±14.75	10.1±1.52	20.9±1.45	17.1±1.39	<0.001*
	Range	28.1 - 30.3	8.3 - 12	18.9 - 22.3	15.5 - 18.8	
Post hoc		P1	<0.001*	<0.001*	0.001*	
		P2		<0.001*	<0.001*	
		P3			0.009*	
CAT (U/mg of protein)	Mean ± SD	40.3±2.24	10.1±1.49	23.5±3.9	22.7±1.76	<0.001*

	Control group	Tx group	Tx /Pg group	Tx /La group	Control group	
	Range	37.2 - 42.5	8.4 - 11.8	19.6 - 27.9	20.4 - 24.5	
Post hoc		P1	<0.001*	<0.001*	0.001*	
		P2		<0.001*	<0.001*	
		P3			0.722	

MDA: Malondialdehyde, GSH: glutathione, SOD: Superoxide dismutase, CAT: Catalase, * statistically significant as P-value <0.05. P1: P-value between control group and the remaining groups, P2: P-value between Tx Group and the remaining groups, P3: P-value between Tx /Pg group and the remaining group

Table 2: ANOVA is used to examine the data, which are shown as Mean values ± SD of Area % of Caspase 3 and Area % of Nrf2 in the ovarian tissue and the uterine tissue of control and experimental groups

		Control group	Tx group	Tx /Pg group	Tx /La group	Control group
Ovarian tissue						
Caspase-3 staining	Mean ± SD	1.8±0.59	12±2.53	7±1.02	8.95±2.08	<0.001*
	Range	1.2 - 2.5	8.9-14.6	5.6 - 7.9	6.4-11.4	
Post hoc		P1	<0.001*	<0.001*	0.001*	
		P2		<0.001*	0.122	
		P3			0.144	
Nrf2 staining	Mean ± SD	15.3±0.8	6.5±0.94	17±1.02	17.5±0.86	<0.001*
	Range	14.2 - 16.1	5.4 - 7.6	15.6 - 17.9	16.4 - 18.5	
Post hoc		P1	<0.001*	0.042*	<0.001*	
		P2		<0.001*	<0.001*	
		P3			0.525	
Uterine tissue						
Caspase-3 staining	Mean ± SD	1.71±0.66	16.95±3.16	5.27±1.04	6.67±0.59	<0.001*
	Range	0.67 - 2.5	12.4 - 23.1	3.9 - 6.9	5.9 – 7.5	
Post hoc		P1	<0.001*	<0.001*	0.001*	
		P2		<0.001*	<0.001*	
		P3			0.53	
Nrf2 staining	Mean ± SD	11.05±0.89	5.48±0.43	12.33±0.4	11.27±0.64	<0.001*
	Range	9.8 – 12.5	4.8 – 6.1	11.7 – 12.9	10.5 – 12.4	
Post hoc		P1	<0.001*	<0.001*	0.399	
		P2		<0.001*	<0.001*	
		P3			<0.001*	

* statistically significant as P-value <0.05. P1: P-value between control group and the remaining groups, P2: P-value between Tx Group and the remaining groups, P3: P-value between Tx /Pg group and the remaining group

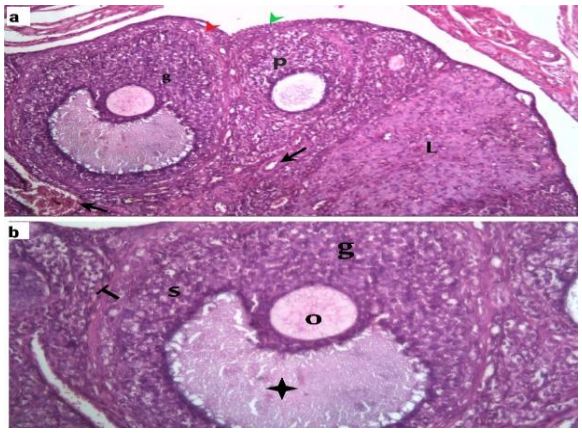

Fig. 1: photomicrographs of control groups rat ovarian sections, revealing

a: normal germinal epithelium (green arrowhead) with an underlying tunica albuginea (red arrowhead). The cortex contains many follicles at different stages of growth as: primary follicles (p), graffian follicle (g) and Corpus luteum (L). Blood vessel (arrow) is observed. (H&E x 100)

b: graffian follicle (g) is formed of an oocyte (O), outer lining of theca cells (T), multiple layers of granulosa cells (s) with presence of antral spaces (star). (H&E x 200)

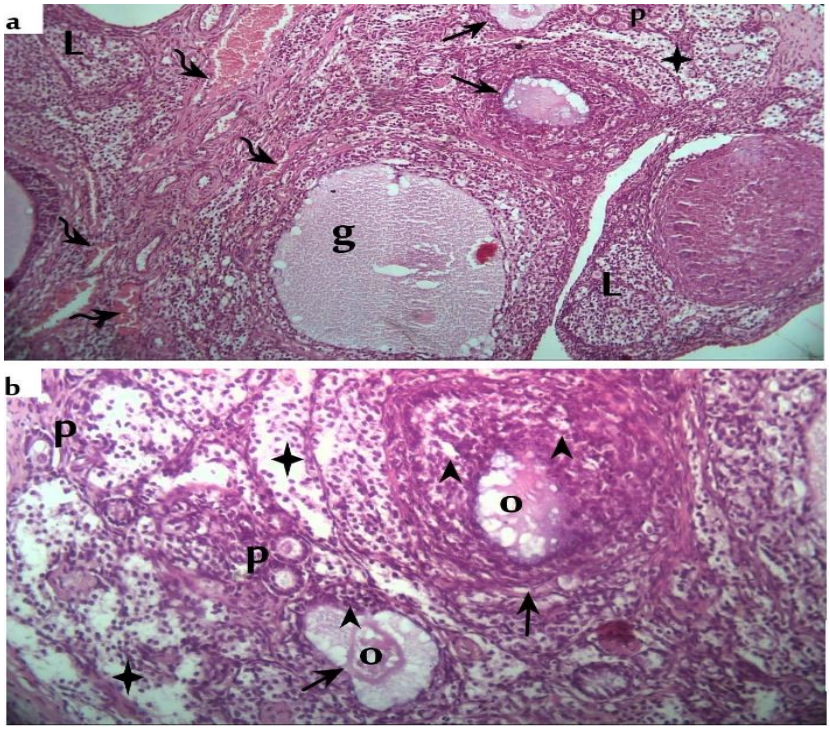

Fig. 2: photomicrographs of rat ovarian sections of Tx group, revealinga: a degenerated atretic primordial (P), secondary follicles (arrow) and graffian follicle (g). Corpus luteum has vacuolated granulosa cells with pyknotic nuclei (L). There is many congested blood capillary (curved arrow) and cortical stromal edema (star). (H&E x 100)b: Atretic secondary follicle (arrow) shows degenerated oocytes (O) with vacuolated granulosa cell with pyknotic nuclei (arrowheads). Notice cortical stromal edema (star) and degenerated atretic primordial (P). (H&E x 200)

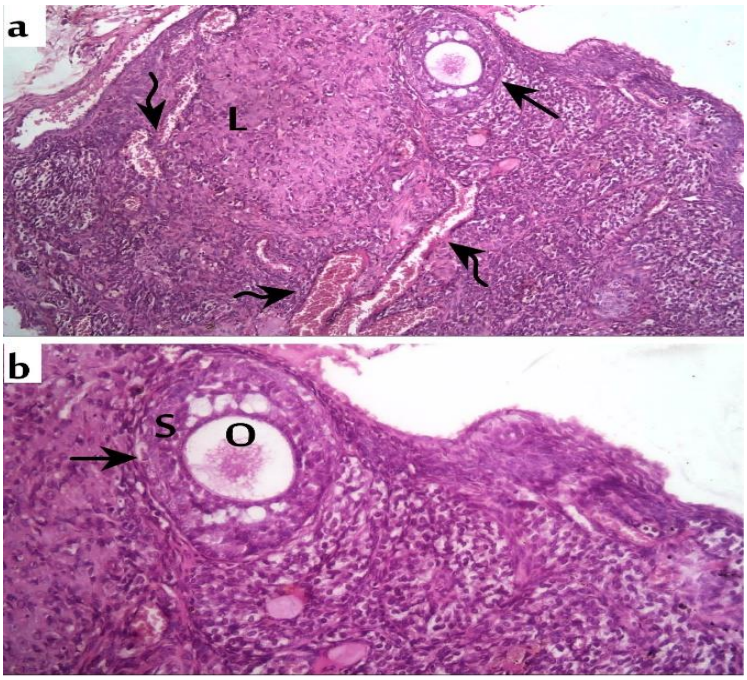

Fig. 3: photomicrographs of rat ovarian section of Tx /Pg group, revealinga: normal secondary (arrow) and corpus luteum (L). There are many congested blood capillaries (curved arrow), and a significant amount of cell infiltration. (H&E x 100)b: normal secondary (arrow) has normal oocyte (O) and lined by normal granulosa cells (s). (H&E x 200)

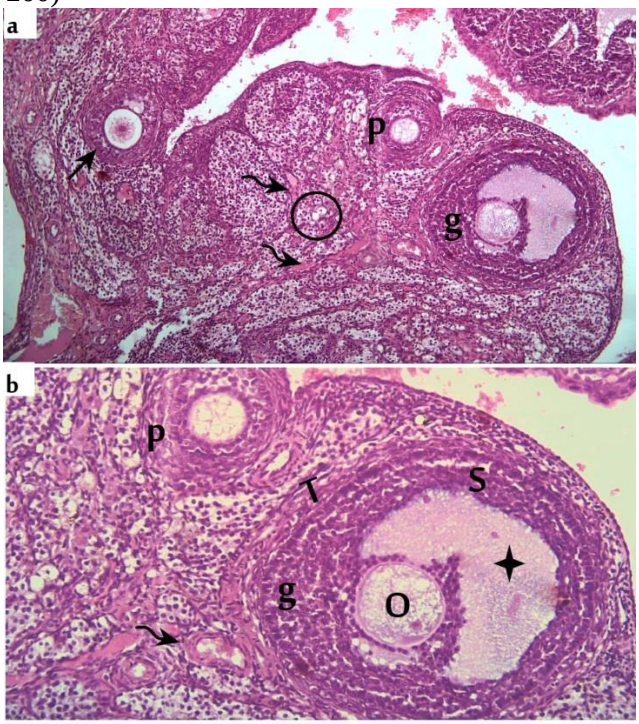

Fig. 4: photomicrographs of rat ovarian sections of Tx /La group, revealing
a: many follicles at different stages of growth as: primary follicles (p), secondary follicle (arrow) and graffian follicle (g). Congested blood vessels (curved arrow) are observed with little interstitial cell vacuolar changes (circle). (H&E x 100) b: graffian follicle (g) is formed of an oocyte (O), outer lining of vacuolated theca interna (T), multiple layers of granulosa cells (s) with presence of antral space (star) filled with secretion. (H&E x 200)

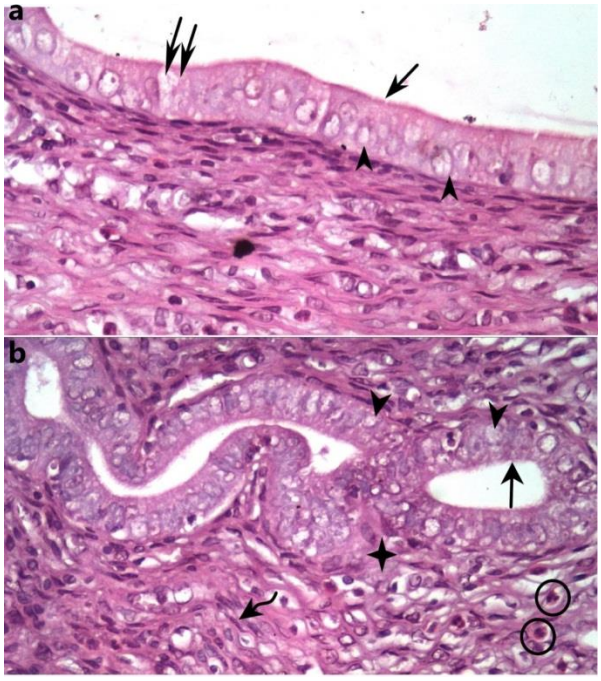

Fig. 5: photomicrographs of control groups rat's the endometrium section, revealing (H&E x 400):

a) The columnar epithelial cells lining the uterine cavity having secretory cytoplasm (double arrows), with vesicular nuclei (arrowhead) and an apical brush border (arrow).
b) Endometrial glands are well-differentiated and encircled by stromal cells. The vesicular nuclei (arrowhead) and apical brush (arrow) can be seen in the glandular epithelial cells. Three different cell types make up stromal cells: leukocytes with a segmented nucleus and deep acidophilic cytoplasm (circle), spindle-shaped cells with darkly pigmented nuclei (curved arrow), and big cells with vesicular nuclei (star).

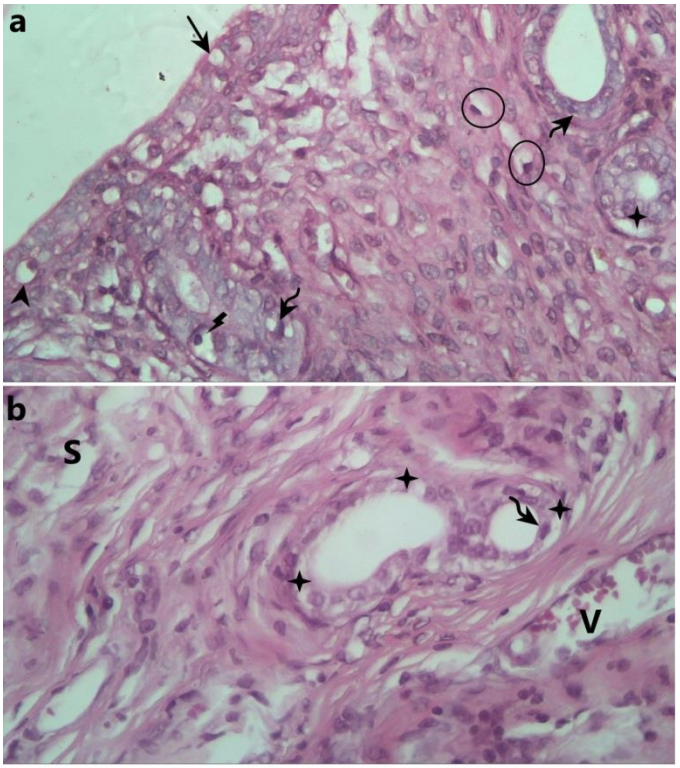

Fig. 6: photomicrographs of the endometrium section of Tx group, revealing (H&E x 400):
a) Cubical epithelial cells with vacuolated nuclei (arrowhead) and cytoplasmic vacuoles (arrow). The stromal cells show darkly stained nuclei with cytoplasmic vacuoles (circle). And glands with apoptotic changes of pyknotic nuclei (curved arrow) or vacuolated nuclei (zigzag) or cytoplasmic vacuoles (star)
b: the stroma shows small glands with cytoplasmic vacuoles (star) and pyknotic nuclei (curved arrow). Congested blood vessel (v) and stromal spaces (s) can also be detected.

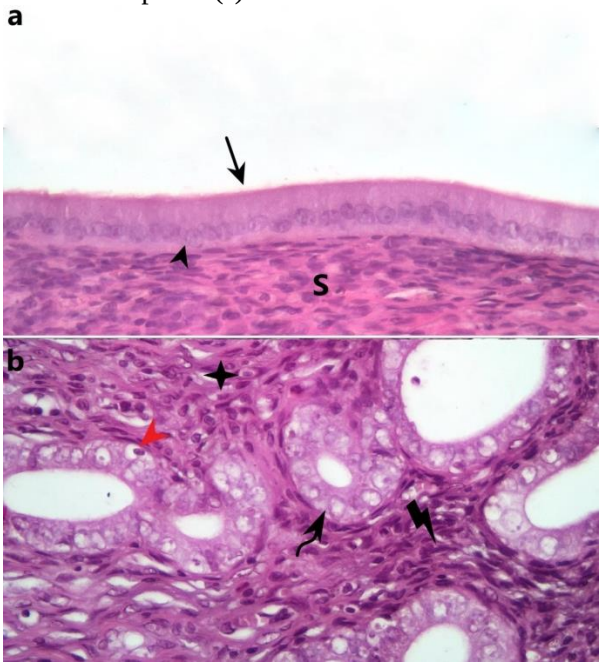

Fig. 7: photomicrographs of the endometrium section of Tx /Pg group, revealing (H&E x 400):

a: The lining epithelium seems to be taller, including vesicular nuclei (arrowhead) and an apical brush border (arrow). The highly cellular stroma (S) can be seen.
b: The epithelial cells lined the gland showed rounded vesicular nuclei (curved arrow). Some cells show dark irregular apoptotic nuclei (red arrowhead). Cells with vesicular nuclei (star) and spindle-shaped nuclei (zigzag) surround the glands.

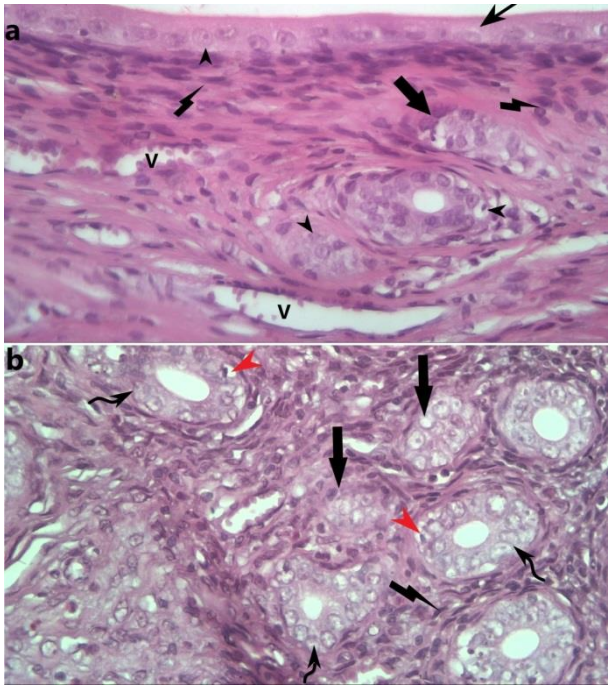

Fig. 8: photomicrographs of the endometrium section of Tx /La group, revealing (H&E x 400):
a: Round vesicular nuclei (head arrow) are seen in the epithelium of the cubical surface (arrow). It shows a dense stroma that is mostly composed of spindle-shaped (zigzag) cells. It is also possible to notice several clogged blood vessels (v). Certain glands appear as solid cell strands (thick arrow).
b: The vesicular nuclei (curved arrows) of the glandular epithelial cells are observed. The nuclei of certain cells are darkly pigmented (red arrowhead). Another gland (thick arrow) is devoid of lumen. The glands are surrounded by many cells with spindle-shaped nuclei (zigzag).

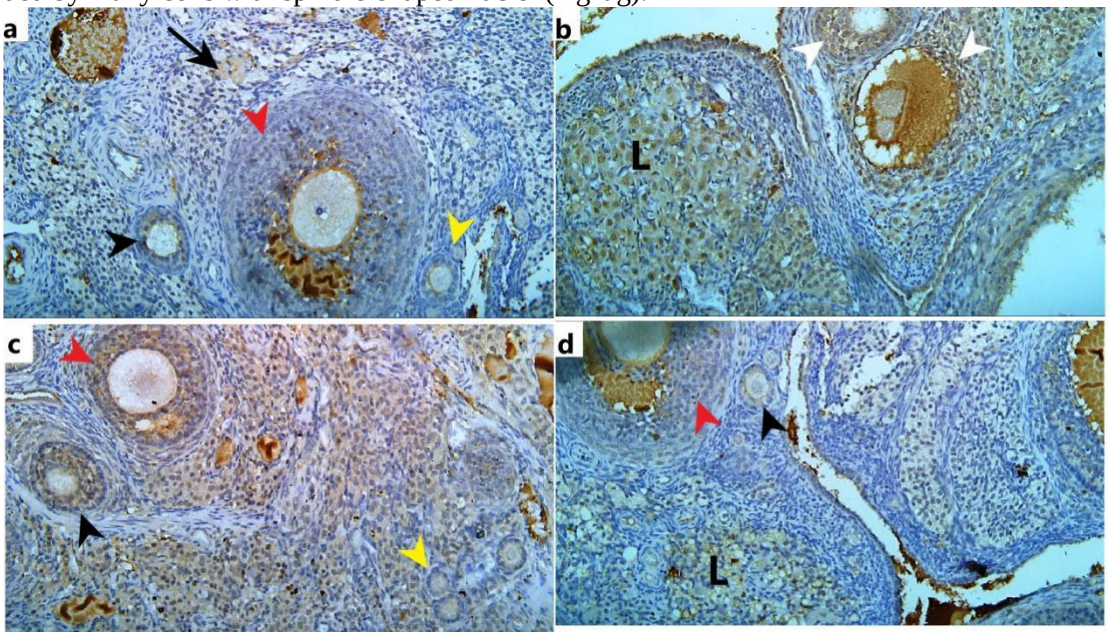

Fig. 9: Photomicrographs of the ovarian sections (Caspase 3 immunohistochemical staining, x 200):
a) Ovarian sections of rats from control groups showed minimal caspase 3 positive in apoptotic cells inside the ovarian tissue, including the medulla (arrow), ovarian cortex, primordial (yellow arrowhead), primary (black arrowhead), and secondary follicles (red arrowhead). b) TX group ovarian sections showed elevated caspase 3 positivity in apoptotic cells seen in the corpus luteum (L) and atretic follicles (white arrowhead). C) Moderate caspase 3 positivity was seen in the apoptotic cells within the ovarian tissues of rats from Tx

/Pg group; these cells included primordial (yellow arrowhead), primary (black arrowhead), and secondary follicles (red arrowhead). d) Rats from Tx /La group ovarian tissues showed lessobvious caspase 3 positive in the ovarian tissueapoptotic cells, both primary (black arrowhead) and secondary follicles (red arrowhead) and corpus luteum (L).

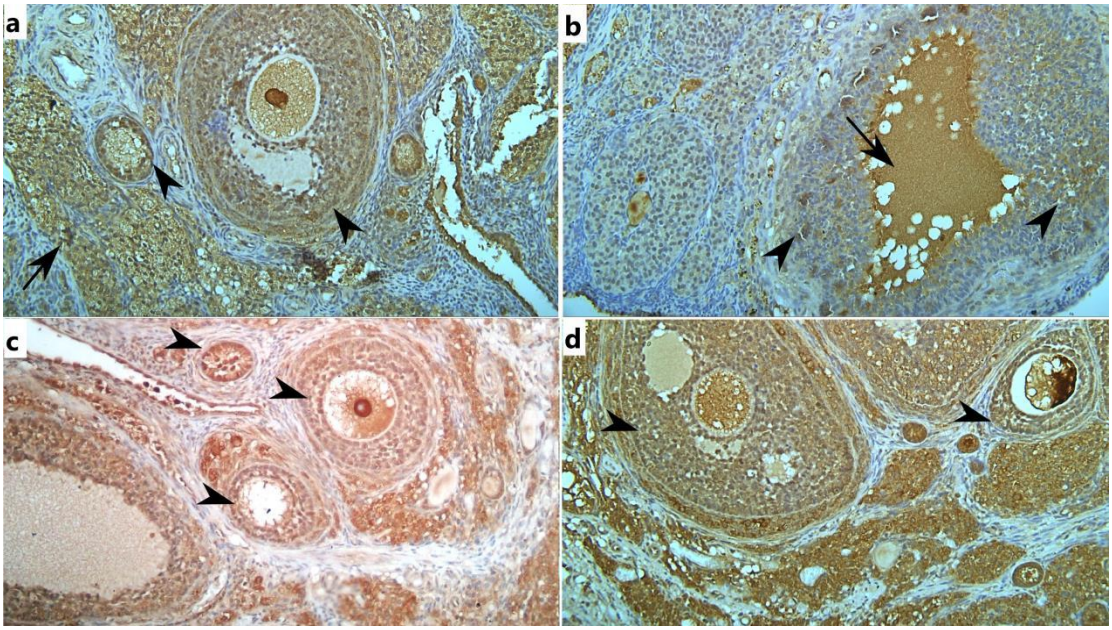

Fig. 10: Photomicrographs of the ovarian sections (Nrf2 immunohistochemical staining, x 200):
(a) Control group shows positive Nrf2 in cytoplasm of granulosa cells (arrowhead) and medulla (arrow). (b) Tx group has low Nrf2 positivity in cytoplasm of granulosa cells (arrowhead) and follicular fluid (arrow). (c) Tx /Pg group shows extensive Nrf2 cytoplasmic positivity in granulosa (arrowhead). (d) Tx /La group shows a positive Nrf2 marked reaction in cytoplasm of granulosa (arrowhead).

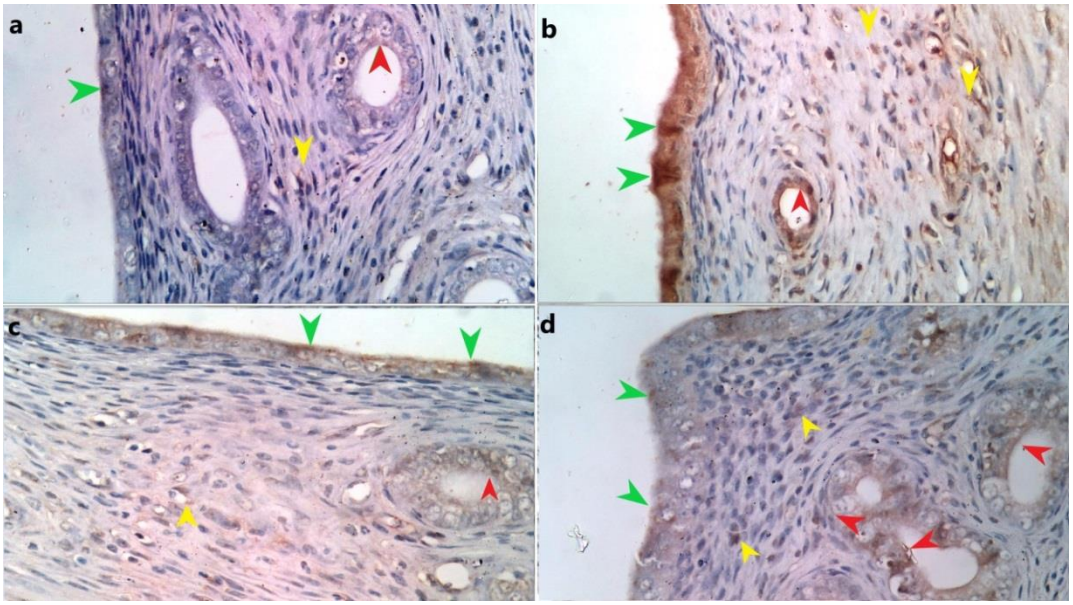

Fig. 11: Photomicrographs of the endometrium (Caspase 3 immunohistochemical staining, x 200):
A) the endometrium from control group featuring low caspase 3 expression in apoptotic cells within the secretory epithelium (green arrowhead), glands (red arrowhead) and stroma (yellow arrowhead) . b) the endometrium from Tx group featuring high caspase 3 expression in the secretory epithelium (green arrowhead), glands (red arrowhead) and stroma (yellow arrowhead). C) The endometrium from Tx /Pg group featuring low caspase 3 expression in the secretory epithelium (green arrowhead), glands (red arrowhead) and stroma (yellow arrowhead). d) the endometrium of rats from Tx /La group featuring less obvious

caspase 3 expression in within the secretory epithelium (green arrowhead), glands (red arrowhead) and stroma (yellow arrowhead).

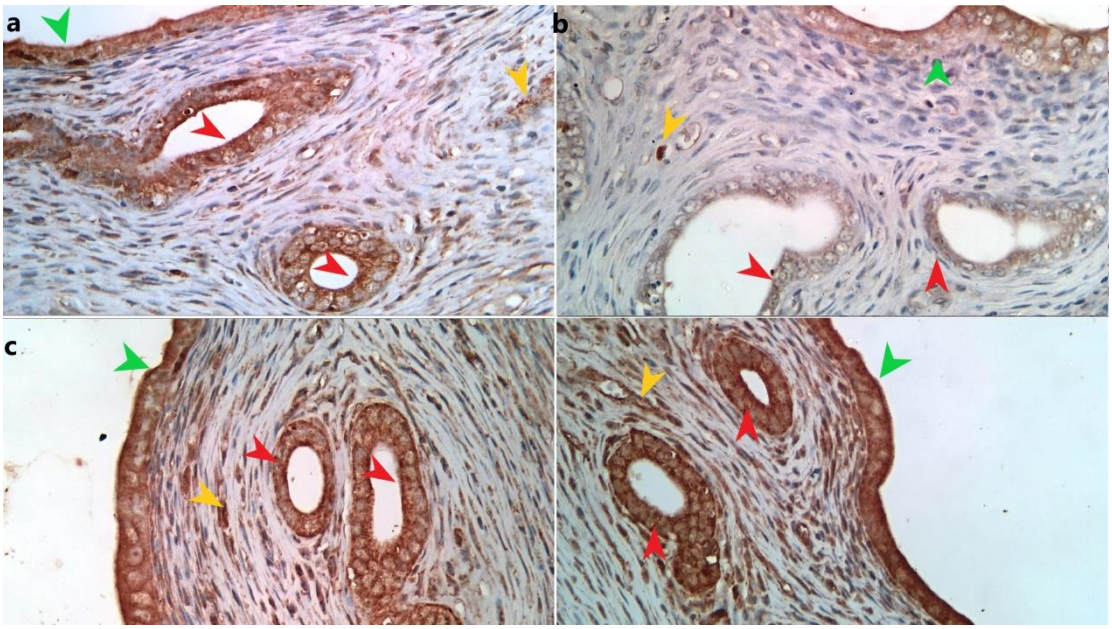

Fig. 12: Photomicrographs of the endometrium (Nrf2 immunohistochemical staining, x 200):
a) the endometrium from control group featuring less obvious Nrf2 positivity in cytoplasm of the secretory epithelium (green arrowhead), glands (red arrowhead) and stroma (yellow arrowhead) . b) the endometrium from Tx group featuring low Nrf2 positivity in cytoplasm of the secretory epithelium (green arrowhead), glands (red arrowhead) and stroma (yellow arrowhead). C, d) The endometrium from Tx /Pg group and Tx /La group respectively featuring increase Nrf2 positivity within the secretory epithelium (green arrowhead), glands (red arrowhead) and stroma (yellow arrowhead).

DISCUSSION:

An imbalance between pro- and antioxidant agents results in cellular and molecular damage that is known as oxidative stress [19]. The kind of oxidant, where and how much it is produced, the role of different antioxidants, and the capacity of the organism repair mechanisms all influence how it affects the body. This occurs in biological systems when there are many reactive oxygen species (ROS) and/or not enough antioxidants [20].

The current study revealed a rise in ovarian and uterine MDA that may have resulted from TMX increased production of ROS [21]. It was also discovered that the histological alterations in the uterine and ovaries were linked to decreased GSH and elevated lipid peroxidation [22]. In this work, oxidative stress and the production of free radicals disrupt the lipids in the cell membrane and this mechanism may be responsible for the the histopathological changes [23].

Superoxide dismutase (SOD) and catalase (CAT), two enzymatic antioxidants, are considered to be the first line of protection against free radicals, acting to neutralize them and prevent their further development [23]. Superoxide radicals are broken down by the SOD enzyme, producing hydrogen peroxide. The CAT enzyme then detoxifies the hydrogen peroxide. Oxidative stress is unquestionably caused by the reduction in cellular SOD and CAT enzymes and the antioxidant GSH [20]. Reduced activity of SOD, CAT, and GSH in the current study indicates that TMX create significant oxidative stress and alter the body systems, leading to ovarian and uterine damage.

L-arginine, on the other hand, was able to improve the effect of TMX exposure by raising CAT and SOD activity and lowering MDA levels. This confirms the results of other studies [25,26,27]that showed the antioxidant action of L-arginine, perhaps via downregulating the expression of miR-221 and upregulating the expression of eNOS and NO generation. By preventing the uncoupling of nitric oxide synthesis and so boosting NO generation, L-arginine has the potential to mitigate TNF-α/IL-6-induced inflammation and reduce oxidative stress [28].

In this study, pycnogenol significantly reduced the MDA level when compared to the Tx group. Furthermore, in comparison to the Tx group, pycnogenol markedly raised the GSH and SOD levels in the Tx /Pg group. It is in the line with a

previous study that demonstrated Pycnogenol antioxidative properties, pretreatment had a protective impact on cisplatin-induced uterine and ovarian damage in rats [12].

As regard the histological finding of Hematoxylin and Eosin stained ovarian sections from rats supplied with TMX, there were changes as presence of atretic follicles, disorganized and vacuolated granulosa layer of developing follicles, the oocyte disappeared, and these results agreed with the findings of earlier research [4].Also the uterine tissue showed abnormal uterine gland with degeneration of its lining epithelium. In addition, there were degenerated endometrial glands, cellular infiltration in the endometrial stroma, and degenerated cells in the uterine endometrial epithelium. It was observed that there was deteriorated endometrial epithelium and circular muscle necrosis infiltrated by lymphocytes with a high percentage of apoptotic figures in rats exposed to TMX [1].

This study demonstrated the improvement of TMX toxicity in the uterine and ovarian tissues by pycnogenol. Numerous surface epithelial cells were tall, columnar, with oval vesicular nuclei and vacuolated cytoplasm, although distinct phases of ovarian follicles were clearly visible with regular structure. Our histological findings were consistent with the finding of prior research; pycnogenol can reduce oxidative stress in the uterine and ovarian tissues caused by cisplatin [12].

In this study, the group that was injected with L-Arginine displayed few apoptotic cells in the ovarian tissue. Moreover, there were interstitial vacuolar changes and congested blood vessels with highly cellular infiltration. L-Arginine was observed to aid in the regeneration of the ovarian tissue and block damage induced by stress and toxicity of Zinc oxide nanoparticles [15]. On the other hand, the group that received L-arginine injection showed almost typical surface epithelium as well as clearly characterized uterine glands in a densely cellular stroma. Utilizing the established human endometrial epithelial cell line RL95-2 as an in vitro model for endometrial cells in humans, the earlier study findings indicate the function of L-arginine in the control of endometrial development and death [29].

Apoptosis is a biological process that is tightly controlled by a variety of pro-and anti-apoptotic proteins. The control of inflammatory cytokines and the production of proteins associated to apoptosis are connected to the toxicological and carcinogenic effects of TMX. Certain apoptotic triggers cause the proenzyme caspase-3 to cleave and activate [30]. This study demonstrated a considerable increase in the positive area % of caspase-3 antibody in ovarian and uterine tissues of TMX-treated rats as compared with the control group. These results align with the conclusions of a study that showed the level of caspase-3 protein in uterine sections of group treated with TMX were elevated by about 4.8 folds and 9.8 folds respectively when compared with control group [1].

L-arginine reduced testicular toxicity in rats exposed to dichlorvos by enhancing male sex hormones and epididymal sperm characteristics and by inhibiting caspase 3 mediated apoptosis in response to oxidative stress [26].Moreover, another study was revealed that pycnogenol pre-treatment protected the hepatoarchitecture of rats from gentamicin -induced damage due to anti-apoptotic effect through reducing Caspase 3 expression [31].

One of the key regulators of the cellular defense system against oxidative damage is Nrf2, a redox-sensitive factor. Its activation initiates downstream antioxidant proteins and phase II detoxifying enzymes [32]. In our study, ovarian and uterine tissues in control group showed larger positive area of Nrf2, but more positive cells were found in ovarian and uterine tissues of rats treated with L-arginine and Pycnogenol compared to ovarian and uterine tissues of TMX treated group. As evidence, TMX treatment markedly increased oxidative stress in the rat brain, and this was due to Nrf2 and its downstream genes being inhibited [33].Furthermore, acetamiprid significantly reduced the expression of Nrf2 in the male rats' kidney tissue [34].However, it was also demonstrated how the antioxidant pycnogenol improved depression, motor function, and the expression of the Nrf2 and NF-kB genes in an experimental model of Parkinson's disease [35].

Arginine has been demonstrated to ameliorate the extension of estrous cycle days, hormone level problems in multiparous Hu sheep, and boost the antioxidant capacity of ovarian tissues because it stimulates the Nrf2/Keap1 pathway [36,37].It has been previously established that the amino acid arginine exhibits antioxidant benefits by upregulating the production of antioxidant products induced by AREs (antioxidant responsive elements) expressions via Nrf2-Keap1 pathway [38].

The therapeutic benefits of L-arginine and Pycnogenol on the ovary and uterine tissue were compared in this study. It is anticipated to offer more trustworthy proof of the combination effectiveness and safety in treating ovarian and uterine toxicity brought on by trimethoxam. According to earlier research, treating elderly

individuals with mild to moderate erectile dysfunction with a combination of pycnogenol and L-arginine significantly improved their sexual performance [39].

CONCLUSION

Providing pycnogenol and L-arginine to rats receiving trimethoxam decreased the ovarian and uterine toxicity.

CONFLICT OF INTEREST

The authors declare no conflict of interest.

FINANCIAL DISCLOSURES

This study was not supported by any source of finding.

REFERENCES

1. El-Din MA, Ghareeb A.E, El-Garawani I.M, El-Rahman H.A. Induction of apoptosis, oxidative stress, hormonal, and histological alterations in the reproductive system of thiamethoxam-exposed female rats. Environ Sci Pollut Res Int.2023; 30 (31), 77917-77930. doi:10.1007/s11356-023-27743-2.
2. Yi L., Zhang S., Chen X., Wang T., Yi X., Yeerkenbieke G. et al. Evaluation of the risk of human exposure to thiamethoxam by extrapolation from a toxicokinetic experiment in rats and literature data. Environ Int. 2023; 173, 107823-33.doi: 10.1016/j.envint.2023.
3. Wang YingHuan W. Y., Zhang Yang Z. Y., Zeng Tao Z. T., Li Wei L. W., Yang Lu Y. L., Guo BaoYuan, G. B. Accumulation and toxicity of thiamethoxam and its metabolite clothianidin to the gonads of Eremias argus. 2019; 667, 586-593. doi:10.1016/j.scitotenv.2019.02.419.
4. Liu Y., He Q. K., Xu Z. R., Xu C. L., Zhao S. C., Luo Y. S., et al. Thiamethoxam exposure induces endoplasmic reticulum stress and affects ovarian function and oocyte development in mice. J Agric Food Chem. 2021; 69(6), 1942-1952. https://doi.org/10.1021/acs.jafc.0c06340
5. Casillas A., De la Torre A., Navarro I., Sanz P., de los Ángeles Martínez M. Environmental risk assessment of neonicotinoids in surface water. Science of the Total Environment 2022; 809, 151161-75. doi:10.1016/j.scitotenv.2021.151161.
6. Loser D., Grillberger K., Hinojosa M.G., Blum J., Haufe Y., Danker T. et al. Acute effects of the imidacloprid metabolite desnitro-imidacloprid on human nACh receptors relevant for neuronal signaling. Arch Toxicol 2021; 95, 3695–3716. https://doi.org/10.1007/s00204-021-03168-z
7. Bešlo D., Golubić N., Rastija V., Agić D., Karnaš M., Šubarić D., Lučić B. Antioxidant activity, metabolism, and bioavailability of polyphenols in the diet of animals. Antioxidants 2023; 12(6), 1141-53. doi: 10.3390/antiox12061141.
8. Alsawaf S., Alnuaimi F., Afzal S., Thomas R. M., Chelakkot A. L., Ramadan W. S. et al. Plant flavonoids on oxidative stress-mediated kidney inflammation. Biology 2022; 11(12), 1717-28. doi:10.3390/biology11121717.
9. Yi-Ling C, Lin J, Hammes H, Zhang C. "Flavonoids in Treatment of Chronic Kidney Disease" Molecules 2022; 27, 7: 2365-74. doi:10.3390/molecules27072365.
10. Eryilmaz A., Eliyatkin N., Demirci B., Basal Y., Kurt Omurlu I., Gunel C. et al. Protective effect of Pycnogenol on cisplatin-induced ototoxicity in rats. Pharmaceutical biology 2016; 54(11), 2777-2781.doi: 10.1080/13880209.2016.1177093.
11. Ozoner B., Yuceli S., Aydin S., Yazici G. N., Sunar M., Arslan Y. K. et al. Effects of pycnogenol on ischemia/reperfusion-induced inflammatory and oxidative brain injury in rats. Neuroscience letters 2019; 704, 169-175. doi: 10.1016/j.neulet.2019.04.010.
12. Turkler C., Kiremitli T., Onat T., Yildirim E., Yazici G. N., Mammadov R., Sunar M. Can pycnogenol prevent cisplatin-induced damage in uterus and ovaries?. AMS 2022; 18(5), 1364-70. doi: 10.5114/aoms.2019.90414.
13. Taner G., Aydın S., Bacanlı M., Sarıgöl Z., Şahin T., Başaran A. A., Başaran N. Modulating effects of pycnogenol® on oxidative stress and DNA damage induced by sepsis in rats. Phytotherapy Research 2014; 28(11), 1692-1700. doi: 10.1002/ptr.5184.
14. Magdy M. T., EL-Ghareeb A. E. W. A., Attaby F. A., Abd El-Rahman H. A. Assessment of nano-iron particles impact on the reproductive health of female Wistar rats. Beni-Suef Univ J Basic Appl Sci. 2022; 11(1), 93-104. doi:10.1186/s43088-022-00274-4.
15. Efendic F., Sapmaz T., Canbaz H. T., Pence H. H., Irkorucu O. Histological and biochemical apoptosis changes of female rats′ ovary by Zinc oxide nanoparticles and potential protective effects of L-arginine: Ann Med Surg (Lond). 2022; 74-85. doi: 10.1016/j.amsu.2022.103290.
16. Bradford M. M. A rapid and sensitive method for the quantitation of microgram quantities of protein utilizeing the principle of protein-dye binding. Anal Biochem. 1976; 72(1-2), 248-254. doi: 10.1006/abio.1976.9999.
17. Bancroft, J. D., & Layton, C. Connective and mesenchymal tissues with their stains. Bancroft's Theory and practice of histological techniques 2012; 187-214. https://doi.org/10.1016/C2015-0-00143-5.
18. Jakkson P., Blqthe D. Immunohistochemical performances [chapter 8]. Theory and run-through of histological techniques. 7th ed. Philadelphia:

Churchill Livingstone of Elsevier 2013; 267-376. https://doi.org/10.1016/C2015-0-00143-5

19. Tan B. L., Norhaizan M. E., Liew W. P. P., Sulaiman Rahman H. Antioxidant and oxidative stress: a mutual interplay in age-related diseases. Front. Pharmacol. 2018; 9, 1162-73. doi: 10.3389/fphar.2018.01162.
20. El-Garawani I. M., Khallaf E. A., Alne-Na-Ei A. A., Elgendy R. G., Sobhy H. M., Khairallah A., et al. The effect of neonicotinoids exposure on Oreochromis niloticus histopathological alterations and genotoxicity. Bull Environ Contam Toxicol 2022; 109(6), 1001-1009. https://doi.org/10.1007/s00128-022-03611-6
21. Kapoor U., Srivastava M. K., Srivastava L. P. Toxicological impact of technical imidacloprid on ovarian morphology, hormones and antioxidant enzymes in female rats. Food Chem Toxicol. 2011; 49(12), 3086-3089. doi: 10.1016/j.fct.2011.09.009.
22. El-Hak H. N. G., Al-Eisa R. A., Ryad L., Halawa E., El-Shenawy N. S. Mechanisms and histopathological impacts of acetamiprid and azoxystrobin in male rats. Environ Sci Pollut Res Int. 2022; 29(28), 43114-43125. doi: 10.1007/s11356-021-18331-3.
23. Alchalabi A. S., Rahim H., Aklilu E., Al-Sultan I. I., Malek M. F., Ronald S. H., Khan M. A. Histopathological changes associated with oxidative stress induced by electromagnetic waves in rats' ovarian and uterine tissues. Asian Pacific Journal of Reproduction 2016; 5(4), 301-310. doi: 10.1016/j.apjr.2016.06.008.
24. Ra K., Park S. C., Lee B. C. Female reproductive aging and oxidative stress: mesenchymal stem cell conditioned medium as a promising antioxidant. Int J Mol Sci.2023; 24(5), 5053-60 doi:10.3390/ijms24055053.
25. Akhigbe R. E., Afolabi O. A., Ajayi A. F. L-Arginine abrogates maternal and pre-pubertal codeine exposure-induced impaired spermatogenesis and sperm quality by modulating the levels of mRNA encoding spermatogenic genes. Frontiers in Endocrinology 2023; 14, 1180085-92. doi: 10.3389/fendo.2023.1180085.
26. Saka W. A., Adeogun A. E., Adisa V. I., Olayioye A., Igbayilola Y. D., Akhigbe R. E. L-arginine attenuates dichlorvos-induced testicular toxicity in male Wistar rats by suppressing oxidative stress-dependent activation of caspase 3-mediated apoptosis. Biomed Pharmacother. 2024; 178, 117136-44. doi: 10.1016/j.biopha.2024.117136
27. Abdel-Rhman A., Morsy W., Selim N., Abdel-Hady E. A. L-arginine supplementation attenuates ovarian oxidative stress in female rats subjected to chronic intermittent hypoxia. Physiol Int. 2023; 110(4), 326-341. doi: 10.1556/2060.2023.00257.
28. Zhang H., Wang L., Peng F., Wang X., Gong H. L- arginine ameliorates high- fat diet- induced atherosclerosis by downregulating miR- 221. BioMed Research International 2020; (1), 4291327-37. doi.org/10.1155/2020/4291327
29. Greene J. M., Feugang J. M., Pfeiffer K. E., Stokes J. V., Bowers S. D., Ryan P. L. L-arginine enhances cell proliferation and reduces apoptosis in human endometrial RL95-2 cells. Reprod Biol Endocrinol 2013; 11, 1-11. doi: 10.1186/1477-7827-11-15.
30. Li Q., Kobayashi M., Kawada T. Carbamate pesticide-induced apoptosis in human T lymphocytes. Int. J. Environ. Res. Public Health 2015; 12(4), 3633-3645.doi.org/10.3390/ijerph120403633
31. Metin T. O. Hepatoprotective effect of pycnogenol in gentamicin-induced liver injury in rats. Ann Med Res. 2023; 30(3), 370–374. doi:10.5455/annalsmedres.2022.12.399.
32. Yuan X., Fu Z., Ji P., Guo L., Al-Ghamdy A. O., Alkandiri A. et al. Selenium nanoparticles pre-treatment reverse behavioral, oxidative damage, neuronal loss and neurochemical alterations in pentylenetetrazole-induced epileptic seizures in mice. International Journal of Nanomedicine 2020; 6339-6353. doi: 10.2147/IJN.S259134.
33. Habotta O, Ateya A, Saleh RM, El-Ashry ES. Thiamethoxam evoked neural oxido-inflammatory stress in male rats through modulation of Nrf2/NF-kB/iNOS signaling and inflammatory cytokines: Neuroprotective effect of Silymarin. Neurotoxicology. 2023 May; 96:28-36. doi: 10.1016/j.neuro.2023.03.004.
34. Alhusaini A., Fadda L. M., Ali H. M., Hasan I. H., Ali R. A., & Zakaria E. A.. Mitigation of acetamiprid—Induced renotoxicity by natural antioxidants via the regulation of ICAM, NF-kB and TLR 4 pathways. Pharmacol. Rep 2019; 71, 1088-1094. https://doi.org/10.1016/j.pharep.2019.06.008
35. Jafari F., Goudarzvand M., Hajikhani R., Qorbani M., Solati J. Pycnogenol ameliorates motor function and gene expressions of NF-ƙ B and Nrf2 in a 6-hydroxydopamine-induced experimental model of Parkinson’s disease in male NMRI mice. Naunyn-schmiedeberg's Archives of Pharmacology. 2022; 395(3), 305-313. doi: 10.1007/s00210-022-02201-x.
36. Ma Y., Guo Z., Wu Q., Cheng B., Zhai Z., Wang Y. Arginine enhances ovarian antioxidant capability via Nrf2/Keap1 Pathway during the Luteal Phase in Ewes. Animals 2022; 12(16), 2017-23. doi: 10.3390/ani12162017.

37. Guo Y. X., Nie H. T., Xu C. J., Zhang G. M., Sun L. W., Zhang T. T., et al. Effects of nutrient restriction and arginine treatment on oxidative stress in the ovarian tissue of ewes during the luteal phase. Theriogenology 2018; 113, 127-136. . doi.org/10.1016/j.theriogenology.2018.02.016
38. Liang M., Wang Z., Li H., Cai L., Pan J., He H. et al. L. l-Arginine induces antioxidant response to prevent oxidative stress via stimulation of glutathione synthesis and activation of Nrf2 pathway. Food Chem Toxicol. 2018; 115, 315-328. doi: 10.1016/j.fct.2018.03.029
39. Tian Y., Zhou Q., Li W., Liu M., Li Q., Chen Q. Efficacy of L-arginine and Pycnogenol® in the treatment of male erectile dysfunction: a systematic review and meta-analysis. Frontiers in Endocrinology 2023; 14, 1211720-34. doi.org/10.3389/fendo.2023.1211720

Citation

Gad, S., abdow, M. Modulatory effects of pycnogenol and L-arginine on the uterine and ovarian histological alterations provoked by Thiamethoxam in Adult rat model. *Zagazig University Medical Journal*, 2025; (515-530): -. doi: 10.21608/zumj.2024.318727.3566